Insights into Poisoning Mechanism of Zr by First Principle Calculation on Adhesion Work and Adsorption Energy between TiB$_2$, Al$_3$Ti, and Al$_3$Zr

Jianqiang Wu [1], Qilin Ruan [1], Simin Chen [1], Chuanchao Meng [1], Zhengbing Xu [1], Chunhua Wei [1], Hongqun Tang [1,*] and Junsheng Wang [2,3,*]

[1] Guangxi Key Laboratory of Processing for Nonferrous Metals and Featured Materials, Center of Ecological Collaborative Innovation for Aluminium Industry in Guangxi, School of Resources, Environment and Materials, Guangxi University, Nanning 530004, China; w1249433210@163.com (J.W.); CQPSRuanQiLin@163.com (Q.R.); a1321039179@163.com (S.C.); 15216729719@163.com (C.M.); xuzhb@gxu.edu.cn (Z.X.); 20150071@gxu.edu.cn (C.W.)

[2] School of Materials Science and Engineering, Beijing Institute of Technology, Beijing 100081, China

[3] Advanced Research Institute of Multidisciplinary Science, Beijing Institute of Technology, Beijing 100081, China

* Correspondence: hqtang@gxu.edu.cn (H.T.); junsheng.wang@bit.edu.cn (J.W.)

Abstract: Al-Ti-B intermediate alloys are widely used as grain refiners in aluminum alloys owing to the presence of Al$_3$Ti and TiB$_2$ phases. However, the existence of Zr in aluminum alloy melts often results in coarse grain size, leading to Al-Ti-B failure called Zr poisoning. There are three kinds of poisoning mechanisms related to TiB$_2$, Al$_3$Ti, and a combination of TiB$_2$ and Al$_3$Ti for Zr. First, Zr forms ZrB$_2$ or Ti$_2$Zr with TiB$_2$ in Al-Ti-B to reduce the nucleation ability. Second, Zr existing in the aluminum melt with a high melting point Al$_3$Zr then attracts Ti to reduce the dispersion of Ti as a growth inhibitor. Third, Zr reacts with Al$_3$Ti on TiB$_2$ surface to form Al$_3$Zr, thereby increasing the degree of mismatch with Al and diminishing the refiner's ability as a nucleation substrate. To gain a better understanding of the mechanism of Zr poisoning, the first principle was used in this study to calculate the adhesion works (ZrB$_2$//Al$_3$Ti), (Ti$_2$Zr//Al$_3$Ti), (Al$_3$Zr//Al$_3$Ti), (Al$_3$Ti//Al), (TiB$_2$//Al$_3$Zr), and (Al$_3$Zr//Al), as well as the surface energy of Al$_3$Zr and adsorption energies of Al to Al$_3$Ti or Al$_3$Zr. The results demonstrated that Zr poisoning originated from the second guess. Zr element exiting in aluminum melt led to the formation of an Al$_3$Zr (001) surface. The interfacial adhesion work of Al$_3$Zr (001)//Al$_3$Ti (001) was not weaker than that of TiB$_2$//Al$_3$Ti. As a result, Al$_3$Zr first combined with Al$_3$Ti to significantly decline the adsorption of Al$_3$Ti (001) on Al, losing its role as a nucleating agent and grain coarsening. Overall, to prevent failure of the grain refiner in Zr containing aluminum melt, the adhesion work interface between the generated phase of the grain refiner and Al$_3$Zr must remain lower to avoid the combination of the generated phase of grain refiner with Al$_3$Zr. In sum, these findings look promising for evaluating future effects of grain refinement in Zr containing aluminum melt.

Keywords: first principles calculation; adhesion work; adsorption energy; grain refiner; Zr poisoning mechanisms

1. Introduction

Aluminum is a metal with lower cost and lighter weight, thereby widely used in furniture, automobile, aerospace, and navigation. However, higher strength and toughness aluminum alloys are increasingly required for various practical applications. In this regard, grain refinement could be used to improve the microstructure, strength, and toughness of aluminum alloys, as well as reduce defects like component segregation, shrinkage porosity, and cracking.

Among refiners, Al-5Ti-1B is widely used in various fields. With the progress of time, three nucleation mechanisms take place: boride particle theory, peritectic reaction theory, and double nucleation theory [1,2]. Meanwhile, TiB_2 employed as a heterogeneous core with a high melting point possesses an orientation relationship between TiB_2 (0001)//Al (111) and Al. In this respect, Cibula et al. [3] proposed the boride particle theory with TiB_2 as the main nucleation core. By comparison, the peritectic reaction theory mainly considers Al_3Ti phase precipitated in the refiner as the nucleation core. For instance, Crossley et al. [4] proposed a peritectic reaction (L + Al_3Ti → α- Al) nucleation. However, both theories suffer from defects. For example, Gru'zleski et al. [5] directly added large amounts of TiB_2 particles to the melt and noticed the possible exclusion of TiB_2 toward the aluminum grain boundary, showing TiB_2 is not the main nucleating material. On the other hand, Ti content introduced into the refiner often does not reach 0.01 wt.%, thereby preventing the occurrence of peritectic reactions due to the very far lower Ti content than the level of peritectic reaction. The latest theory has to do with the dual nucleation theory, suggesting the formation of a thin layer of Al_3Ti on the TiB_2 surface. In this regard, Jones et al. [6] reported the easy segregation of Ti on TiB_2 surface by calculating the chemical formula in the melt. Qi et al. [7] noticed higher Ti content around TiB_2 in the refined aluminum alloy than that around TiB_2 in the refiner. Fan et al. [8] observed two-dimensional Al_3Ti by transmission electron microscopy. Schumacher et al. [9] recorded coating of a TiB_2 surface with Al_3Ti by transmission imaging after adding the refiner to aluminum-based glass alloy, further confirming the reliability of the double nucleation theory.

For aluminum alloys containing Zr, the effect of Al-5Ti-1B refiner would be significantly reduced [10]. Some studies dealing with Zr poisoning have so far been reported, and three kinds of Zr poisoning mechanisms have been recorded: targeting TiB_2, Al_3Ti and (TiB_2//Al_3Ti). Jones and Pearson suggested the association between Zr and TiB_2. They first proposed the replacement of Ti atoms by Zr on a TiB_2 surface in combination with boride particle theory. Under these conditions, ZrB_2 was also formed on TiB_2 surface, thereby affecting the ability of TiB_2 as a nucleation substrate. Wang et al. also noticed the associated Zr to TiB_2 and confirmed the dual nucleation theory through transmission imaging by observing Zr atoms on TiB_2 refiner surface in Al alloys containing Zr with Ti_2Zr formed on the surface. In this case, Zr may have caused the dissolution of Al_3Ti bimetallic compounds formed on the surface of TiB_2. Johnsson et al. [11] employed the peritectic reaction theory to propose Zr poisons free Al_3Ti in the melt, as well as a combination of Al_3Ti with Al_3Zr forming ternary compounds. The last kind of guess consisted of Zr poisoning (TiB_2//Al_3Ti), where Zr reacted with Al_3Ti thin layer on the TiB_2 surface, and Zr replaced Ti atom in Al_3Ti.

In the present study, vasp program was used to carry out calculations. For dual nucleation theory, calculations corresponding to three kinds of guesses for Zr poisoning mechanisms were performed. The first consisted of an Al melt without Zr: TiB_2 (0001)//Al_3Ti (112), Al_3Ti (112)//Al (111). The second dealt with Zr poisoning TiB_2 by calculating the works of TiB_2-ZrB_2 (0001)//Al_3Ti (112) and TiB_2-Ti_2Zr (0001)//Al_3Ti (112). The third had to do with Zr adsorption free Ti, where the minimum energy surface of Al_3Zr was first calculated followed by Al_3Ti (112)//Al_3Zr (114) and Al_3Ti (001)//Al_3Zr (001). Fourth, Zr poisoned Al_3Ti on a TiB_2 surface was explored by calculating TiB_2 (0001)//Al_3Ti-Al_3Zr (112) and TiB_2 (0001)//Al_3Zr (114). Finally, calculations related to Al_3Ti and Al_3Zr in contact with an Al melt were performed, including Al_3Ti (001)//Al (001), Al_3Zr (001)//Al (001), Al_3Ti-Al_3Zr (112)//Al (111), and Al_3Zr (114)//Al (111). Note that Al atoms were adsorbed by Al_3Ti and Al_3Zr.

The three kinds of guesses for the Zr poisoning mechanism and the first principle calculations are summarized in Table 1.

Table 1. The three kinds of guesses for Zr poisoning mechanism and the first principle calculations.

Zr Poison Target	Toxic Products	Adhesion Work Calculation	Adsorption Energy Calculation
Not containing Zr in Aluminum melt		TiB_2 (0001)//Al_3Ti (112) Al_3Ti (112)//Al (111)	Al_3Ti (112) adsorbed Al
TiB_2	ZrB_2 Ti_2Zr	TiB_2-ZrB_2 (0001)//Al_3Ti (112) TiB_2-Ti_2Zr (0001)//Al_3Ti (112)	
Free Al_3Ti	(Al_3Ti//Al_3Zr)	Al_3Ti (001)//Al_3Zr (001) Al_3Ti (001)//Al (001) Al_3Zr (001)//Al (001) Al_3Ti (112)//Al_3Zr (114)	Al_3Ti (001) adsorbed Al Al_3Zr (001) adsorbed Al
Al_3Ti on TiB_2 surface	(TiB_2//Al_3Zr)	TiB_2 (0001)//Al_3Ti-Al_3Zr (112) Al_3Ti-Al_3Zr (112)//Al (111) TiB_2 (0001)//Al_3Zr (114) Al_3Zr (114)//Al (111)	Al_3Zr (114) adsorbed Al

2. Computing Method

2.1. First Principle

All simulations in this paper were carried out by vasp5.4 package. To this end, crystal models of various compounds were first established with interface cut by Material studio software. Next, TiB_2 (0001), Al_3Ti (112), Al (111), and other surfaces were all obtained, and vasp package was optimized to yield stable structures and surface energies. Further calculations were then carried out under stable structures, and the atomic adsorption calculations were performed on the surface followed by calculations of adhesion works at the interfaces.

The wave function was generated by the program itself, and charge density was induced by superimposing charges using the conjugate gradient method. The self-consistent convergence energy was set to 1E-5, the pseudo-potential was PBE, and truncation energy was 1.0~1.3 times the energy of the highest pseudo-potential of elements in the compound. The vacuum layer thickness adopted a height of 15 Å, and the interface was calculated by the relaxation method. The adsorption calculations were based on the method of relaxing the upper three layers and fixing the lower three layers.

2.2. Adhesion Work

The adhesion work can be defined as the energy required to separate the interface and the reversible work per unit area required to separate the X and Y condensed phase interface to generate two free surfaces. The adhesion work can mainly be reflected in the stability and bonding ability between the two interfaces, where bigger energies would yield more stability. The calculation formula can be expressed by Equation (1):

$$W_{ab} = (E_{XY} - E_X - E_Y)/A \tag{1}$$

where E_{XY} represents the total interface energy when X is combined with Y, E_X and E_Y are, respectively, the total surface energies of surfaces X and Y, and A refers to the area of the contact surface [12,13].

2.3. Surface Energy

Surface energy can be defined as the energy required to create the surface of matter. In the melt, lower energy required to form the surface would lead to the easy spontaneous formation of the surface. This can be calculated according to Equation (2):

$$E_{surf} = (E_{slab} - N_i E_{ibulk})/2A \tag{2}$$

where E_{slab} represents the total energy of the surface, N_i is the number of i atoms in the structure, E_{ibulk} refers to the average atomic energy of i atoms in the single substance of the structure, and A denotes the surface area [14,15].

2.4. Adsorption Energy

The adsorption energy can be defined as the energy required to adsorb atoms on the surface. This can be calculated according to Equation (3):

$$E_{ads} = E_{all} - E_{surf} - E_{atom} \tag{3}$$

where E_{all} represents the total energy of the adsorption system, E_{surf} is the energy of a clean surface, and E_{atom} refers to the energy of isolated atoms [16,17].

3. Results and Discussion

3.1. Adhesion Work TiB₂ (0001)//Al₃Ti (112) and Al₃Ti (112)//Al (111)

In dual nucleation theory, TiB_2 with a high melting point (2980 °C) was taken as the base core to solidify on TiB_2 surface and form an Al_3Ti thin layer. Next, Al underwent nucleation on Al_3Ti surface to yield the orientation relationship of TiB_2 (0001)//Al_3Ti (112) and Al_3Ti (112)//Al (111). Note that dual nucleation theory was the most accepted nucleation mechanism theory to date. The formation of Al_3Ti thin layer was also confirmed by Fan [8] and Schumacher [9].

As shown in Figure 1, the graph of interface structure revealed TiB_2 (0001), Al_3Ti (112), and Al (111) all with the same atomic arrangement order. Additionally, only small differences in atomic spacing were noticed, suggesting good bonding ability between the interfaces between TiB_2 (0001), Al_3Ti (112), and Al (111).
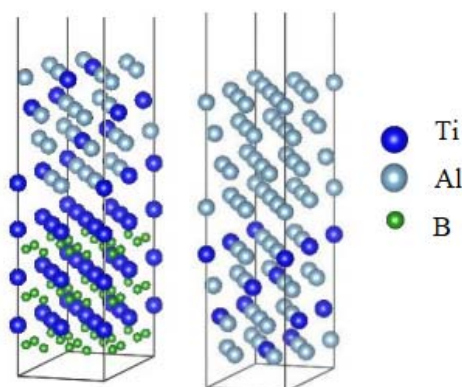

Figure 1. Interfaces of TiB_2 (0001)//Al_3Ti (112) and Al_3Ti (112)//Al (111).

As shown in Table 2, the adhesion work of (TiB_2 (0001)//Al_3Ti (112)) was calculated as -0.228 eV/Å^2, a value much greater than that of (Al_3Ti (112)//Al (111)) (-0.139 eV/Å^2). The binding of Al_3Ti (112) to TiB_2 (0001) was more stable than that of Al_3Ti (112) to Al (111), revealing the experimental formation of Al_3Ti thin layer on TiB_2 surface. Accordingly, the Zr poisoning theory was further studied.

Table 2. The initial and final interface distance, contact area, and adhesion work calculated on TiB_2 (0001)//Al_3Ti (112) and Al_3Ti (112)//Al (111).

Interfaces	Initial d (Å)	W_{AB} (eV/Å^2)	A (Å^2)	Final d (Å)
TiB₂ (0001)//Al₃Ti (112)	3	−0.228	63.82	2.25
Al₃Ti (112)//Al (111)	3	−0.139	55.39	2.31

3.2. Adhesion Work TiB₂-ZrB₂ (0001)//Al₃Ti (112) and TiB₂-Ti₂Zr (0001)//Al₃Ti (112)

The first kind of Zr poisoning guess was mainly aimed to study the action of TiB_2 particles precipitated in the refiner. Jones and Pearson suggested the replacement of Ti by Zr on TiB_2 surface to form ZrB_2, leading to increased degree of mismatch. Wang et al. confirmed dual nucleation theory through transmission imaging, where Zr atoms existing

on TiB_2 surface led to the formation of Ti_2Zr on TiB_2 surface. They believed that Zr caused the dissolution of Al_3Ti on TiB_2 surface. Thus, the interface model was calculated in both cases.

As shown in Figure 2, the left part replaced all Ti ends of TiB_2 surface layer with Zr to yield ZrB_2 surface, while the right part replaced part of Ti with Zr to form a thin Ti_2Zr surface layer. Therefore, the respective values of adhesion work with Al_3Ti were calculated.
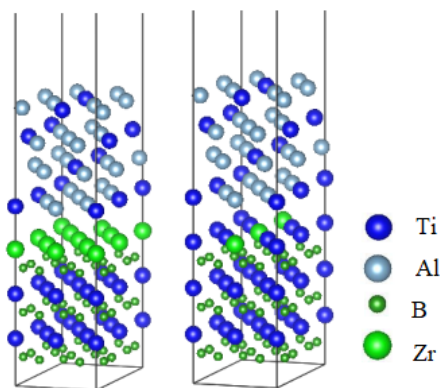

Figure 2. Interfaces of TiB_2-ZrB_2 (0001)//Al_3Ti (112) and TiB_2-Ti_2Zr (0001)//Al_3Ti (112).

As presented in Table 3, the adhesion work between TiB_2-ZrB_2 (0001)//Al_3Ti (112) interface was calculated to -0.226 eV/$Å^2$, and that between TiB_2-Ti_2Zr (0001)//Al_3Ti (112) interface was -0.224 eV/$Å^2$. By replacing Ti on TiB_2 surface with Zr, the binding abilities of ZrB_2 and Ti_2Zr to Al_3Ti decreased slightly by 0.002 eV/$Å^2$ and 0.004 eV/$Å^2$, respectively. However, these reductions were too small to affect the combination with Al_3Ti surface.

Table 3. The initial and final interface distance, contact area, and adhesion work calculated on TiB_2-ZrB_2 (0001)//Al_3Ti (112) and TiB_2-Ti_2Zr (0001)//Al_3Ti (112).

Interfaces	Initial d (Å)	W_{AB} (eV/$Å^2$)	A ($Å^2$)	Final d (Å)
TiB_2-ZrB_2 (0001)//Al_3Ti (112)	3	-0.226	63.82	2.47
TiB_2-Ti_2Zr (0001)//Al_3Ti (112)	3	-0.224	63.82	2.08

3.3. Adhesion Work Al_3Ti (001)//Al_3Zr (001) and Al_3Ti (112)//Al_3Zr (114)

The second kind of poisoning guess proposes Zr poisons-free Al_3Ti in the melt. Since the melting point of Al_3Ti was low, the melting upon addition of Al melt followed gradual precipitation during solidification. In this case, the Ti atoms released by melting could inhibit the growth of Al. In this view, Johnsson et al. [11] proposed that the high melting point Al_3Zr would agglomerate Ti atoms in the melt, as well as reduce the uniform dispersion of Ti in the melt and decline its growth inhibition. Xiao et al. [18] used scanning electron microscopy (SEM) and energy dispersive spectrometry (EDS) techniques to show the bounding and wrapping of Al_3Ti with Al_3Zr on Al_3Zr surface, where Al_3Zr was the core of the aggregate. In this case, Zr poisoning was caused by the combination of Al_3Ti and Al_3Zr to form Al_3 (Zr, Ti).

For precipitation and crystallization of Al_3Zr in the melt with a high melting point, Liu et al. [19] determined the precipitation of $(01\bar{1})$ and (110) in Al_3Zr through transmission electron microscopy (TEM) microstructures and corresponding diffraction patterns. In the present study, multiple modeling and pair screening of Al_3Ti and Al_3Zr crystal planes revealed the existence of (110), (114), and (001) planes of Al_3Zr with the same atomic structure arrangement as Al_3Ti (110), Al_3Ti (112), and Al_3Ti (001) surface, respectively.

The surface of Al_3Zr (110), Al_3Zr (114), and Al_3Zr (001) surface were shown in Figure 3. Since (110), (114), and (001) planes of Al_3Zr were the most easily combined planes with Al_3Ti, a better understanding of which crystal plane Al_3Zr would most likely crystallize or grow in the high-temperature melt can be determined. According to Equation (2),

the surface energies of Al_3Zr (110), (114), and (001) were calculated as -0.008 eV/Å^2, -0.109 eV/Å^2, and -0.136 eV/Å^2, respectively. Hence, Al_3Zr crystallized most easily in (001) plane among the three planes. The second consisted of (114) plane, and the lowest was (110) plane. The energy of (110) plane was close to zero, and its crystallization ability was much lower than those of the other two planes. Hence, Al_3Zr (114) and Al_3Zr (001) surfaces and Al_3Ti were selected to calculate the adhesion capacities.
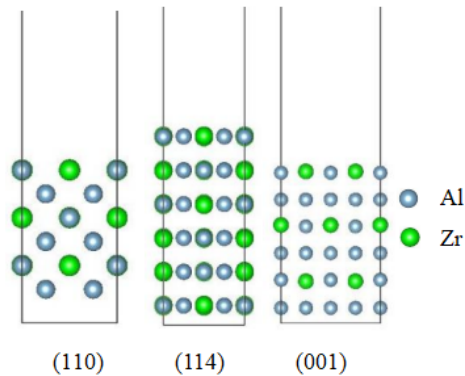

Figure 3. Surfaces of Al_3Zr (110), Al_3Zr (114), and Al_3Zr (001).

The interface of Al_3Ti (001)//Al_3Zr (001) and Al_3Ti (112)//Al_3Zr (114) interfaces were shown in Figure 4. As presented in Table 4, the adhesion works between Al_3Zr (001) and (114) with Al_3Ti were calculated as -0.223 eV/Å^2 and -0.168 eV/Å^2, respectively. The previous calculations of surface energy revealed Al_3Zr (001) surface as the easiest to crystallize in the melt, and its adhesion work with Al_3Ti (001) was calculated to -0.223 eV/Å^2. Compared to the adhesion work between TiB_2 (111) and Al_3Ti (112) surface in the melt, the difference was calculated to be only 0.005 eV, confirming the heterogeneous nucleation of Al_3Zr with a high melting point in the melt to compete with TiB_2 for Al_3Ti. In other words, Al_3Ti would be wrapped on Al_3Zr surface, consistent with the experimental results reported by Xiao et al. [18].
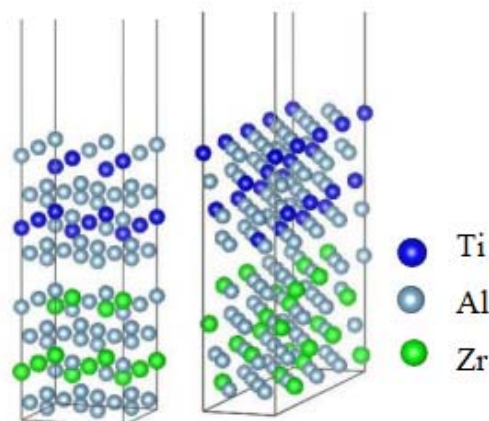

Figure 4. Interfaces of Al3Ti (001)//Al3Zr (001) and Al3Ti (112)//Al3Zr (114).

Table 4. The initial and final interface distance, contact area, and adhesion work calculated on Al_3Ti (001)//Al_3Zr (001) and Al_3Ti (112)//Al_3Zr (114).

Interfaces	Initial d (Å)	W_{AB} (eV/Å^2)	A (Å^2)	Final d (Å)
Al_3Ti (001)//Al_3Zr (001)	3	-0.223	61.00	2.28
Al_3Ti (112)//Al_3Zr (114)	3	-0.168	110.6	2.38

3.4. Adhesion Work TiB$_2$ (0001)//Al$_3$Ti-Al$_3$Zr (112) and TiB$_2$ (0001)//Al$_3$Zr (114)

The third kind of poisoning guess suggested the action of Zr on an Al$_3$Ti thin layer wrapped on a TiB$_2$ surface, and replacement of Ti atoms in Al$_3$Ti by Zr to reduce the effect of Al$_3$Ti. Wang et al. [20] observed the adsorption of Zr atoms on a TiB$_2$ (0001) surface by scanning transmission electron microscopy and showed that Zr may replace Ti of Al$_3$Ti on a TiB$_2$ surface. In the present study, two models were established. The first consisted of Zr replacing the Ti atom of Al$_3$Ti (112) to form Al$_3$Ti-Al$_3$Zr (112), and the second considered Al$_3$Zr (114) surface crystallization on a TiB$_2$ surface.

According to Figure 5 and Table 5, when Zr replaced Ti of Al$_3$Ti (112),the adhesion work between Al$_3$Zr (112) and TiB$_2$ (0001) was calculated to -0.221 eV. This value was 0.007 eV lower than that of TiB$_2$ (0001)//Al$_3$Ti (112) without Zr(as shown in Table 2). The adhesion work of TiB$_2$ (0001)//Al$_3$Zr (114) was 0.027 eV higher than that of TiB$_2$ (0001)//Al$_3$Ti (112). However, the increasing or decreasing range was very small, meaning that the adhesion of Al$_3$Ti and Al$_3$Zr to TiB$_2$ surface was almost the same, meaning that Zr may replace the Ti atom in the representative layer. Meanwhile, the melting point of Al$_3$Zr represented by Zr was higher, making it easier to produce Al$_3$Zr (114) instead of Al$_3$Ti-Al$_3$Zr (112).
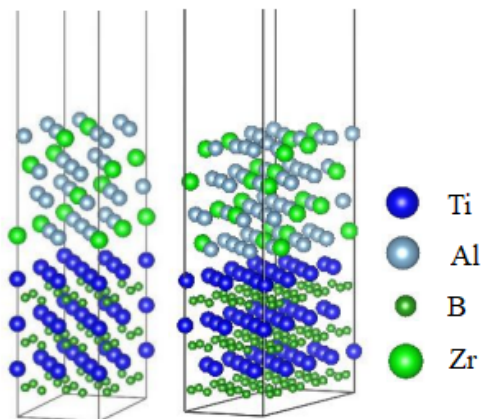

Figure 5. Interfaces of TiB$_2$ (0001)//Al$_3$Ti-Al$_3$Zr (112) and TiB$_2$ (0001)//Al$_3$Zr (114).

Table 5. The initial and final interface distance, contact area, and adhesion work calculated on TiB$_2$ (0001)//Al$_3$Ti-Al$_3$Zr (112) and TiB$_2$ (0001)//Al$_3$Zr (114).

Interfaces	Initial d (Å)	W_{AB} (eV/Å^2)	A (Å^2)	Final d (Å)
TiB$_2$ (0001)//Al$_3$Ti-Al$_3$Zr (112)	3	-0.221	63.82	2.28
TiB$_2$ (0001)//Al$_3$Zr (114)	3	-0.255	110.6	2.22

3.5. Adhesion Work Al$_3$Ti-Al$_3$Zr (112)//Al (111) and Al$_3$Zr (114)//Al (111)

The previous calculations revealed that Zr may replace the Al$_3$Ti thin layer on TiB$_2$ surface. Hence, the adhesion work between Al$_3$Ti-Al$_3$Zr (112) and Al$_3$Zr (114) with Al (111) surface was further calculated to clarify the binding ability with Al from an energetic standpoint.

The interface of Al$_3$Ti-Al$_3$Zr (112)//Al (111) and Al$_3$Zr (114)//Al (111) interfaces were shown in Figure 6. As illustrated in Table 6, the adhesion work of Al$_3$Ti-Al$_3$Zr (112) //Al (111) was 0.002 eV higher than that of Al$_3$Ti (112) //Al (111) (as shown in Table 2). Additionally, the adhesion work of Al$_3$Zr (114) //Al (111) was 0.013 eV lower than that of Al$_3$Ti (112) //Al (111), but the adhesion work of TiB2 (0001) //Al$_3$Zr (114) was higher than that of TiB2 (0001) //Al$_3$Ti (112). Thus, Zr reduced the nucleation ability in Zr-containing alloys, but with a small impact.
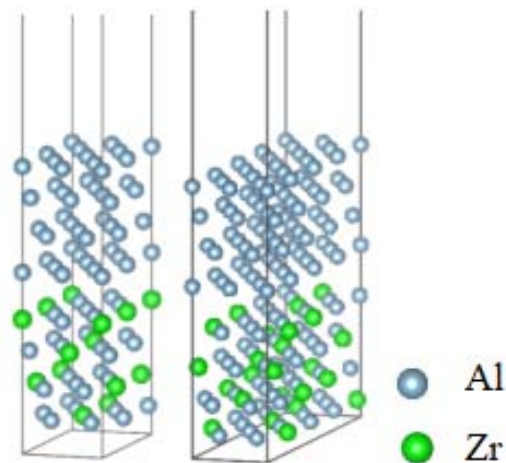
Figure 6. Interfaces of Al$_3$Ti-Al$_3$Zr (112)//Al (111) and Al$_3$Zr (114)//Al (111).

Table 6. The initial and final interface distance, contact area, and adhesion work calculated on Al$_3$Ti-Al$_3$Zr (112)//Al (111) and Al$_3$Zr (114)//Al (111).

Interfaces	Initial d (Å)	W$_{AB}$ (eV/Å^2)	A (Å^2)	Final d (Å)
Al$_3$Ti-Al$_3$Zr (112)//Al (111)	3	−0.141	55.39	2.36
Al$_3$Zr (114)//Al (111)	3	−0.126	110.6	2.39

3.6. Adhesion Work Al$_3$Ti (001)//Al (001) and Al$_3$Zr (001)//Al (001)

The previous calculations mentioned that the presence of Zr element may lead to precipitation of Al$_3$Zr (001) plane crystallization in the melt, as well as the coating of Al$_3$Ti (001) plane on Al$_3$Zr (001) surface. Note that Al$_3$Ti-Al$_3$Zr (112) and Al$_3$Zr (114) were in contact with Al in the melt, while Al$_3$Ti (001) and Al$_3$Zr (001) were in contact with Al. Hence, their adhesion works with Al were calculated.

The Al$_3$Ti (001)//Al (001) and Al$_3$Zr (001)//Al (001) interfaces were shown in Figure 7. According to Table 7, the values of adhesion work between (001) surface of (Al$_3$Ti and Al$_3$Zr) with Al were calculated as −0.140 eV/Å^2 and −0.133 eV/Å^2, respectively. Compared to Al$_3$Ti (112)//Al (111), the difference was also very small, meaning good bonding abilities of Al$_3$Ti(001) and Al$_3$Zr (001) with Al (001).
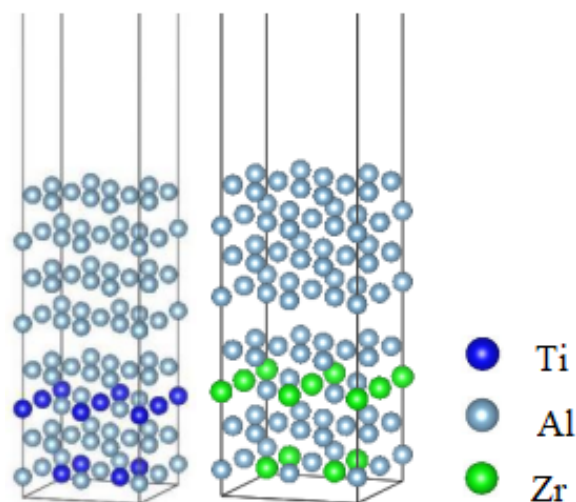

Figure 7. Interfaces of Al$_3$Ti (001)//Al (001) and Al$_3$Zr (001)//Al (001).

Table 7. The initial and final interface distance, contact area, and adhesion work calculated on Al$_3$Ti (001)//Al (001) and Al$_3$Zr (001)//Al (001).

Interfaces	Initial d (Å)	W$_{AB}$ (eV/Å^2)	A (Å^2)	Final d (Å)
Al$_3$Ti (001)//Al (001)	3	−0.140	58.98	2.08
Al$_3$Zr (001)//Al (001)	3	−0.133	64.96	2.09

3.7. Adsorption Energy of Al on Al$_3$Ti (001) or Al on Al$_3$Zr (001)

In addition to the adhesion work used to understand the binding ability between the refiner and Al in the melt, the adsorption energy could also be employed to clarify the adsorption ability of the refiner to Al atoms. The adsorption ability of the refiner to Al atoms in the solute would determine the possible aggregation of Al atoms on its surface to form a new crystal surface. In previous calculations, the second guess of Zr poisoning confirmed the coating of Al$_3$Ti on Al$_3$Zr surface in the melt, with a relationship of site determined as Al$_3$Ti (001)//Al$_3$Zr (001). After surface energy calculations, the adsorption of Al atoms on its stable surface was calculated by considering the adsorption behavior of Al atoms on the surface. As shown in Figure 8, the following four points were considered:
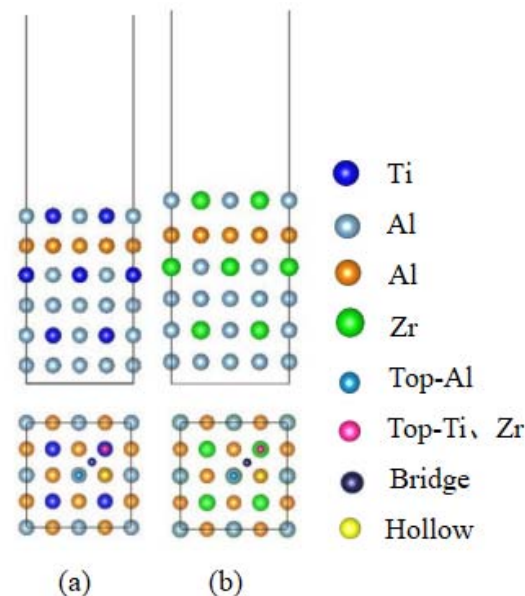

Figure 8. Surface structure and adsorption site of (**a**) Al$_3$Ti (001) and (**b**) Al$_3$Zr (001).

The initial adsorption site and final site of Al$_3$Ti (001) and Al$_3$Zr (001) surfaces were shown in Figure 9. The top sites were all located above the Al atoms, as well as Zr and Ti atoms. Bridge sites were then built between Al-Zr and Al-Ti atoms, and hollows were formed in the center of Al-Zr and Al-Ti quadrilateral. In Figure 9, the adsorption site at the top site remained almost unchanged and stayed at the top site from the beginning to the end of the adsorption process. After completion of the adsorption process of the bridge site, the adsorption site shifted to the top site of the Al atom, while the adsorption site of the hollow site remained unchanged. Both the beginning and end stayed at the hollow site.

Referring to Table 8 for Al$_3$Ti (001) surface, the energy at the hollow site was the most conducive to Al adsorption, with the adsorption energy at the hollow site calculated to −4.664 eV. The Al top site was the second priority adsorption site with an adsorption energy of −4.653 eV. For Al$_3$Zr (001), the Al top site consisted of the highest adsorption energy, thereby the most conducive to the adsorption of Al atoms with the energy of −3.848 eV. The second energy was obtained on the bridge site with a value calculated to −3.845 eV. However, the bridge site moved to the top site after adsorption, and the adsorption energy of Al$_3$Zr (001) for Al atoms was lower than that of Al$_3$Ti (001). This further confirmed that

Al_3Ti could easily attract Al atoms when compared to Al_3Zr, and was thereby better as a core of nucleation.
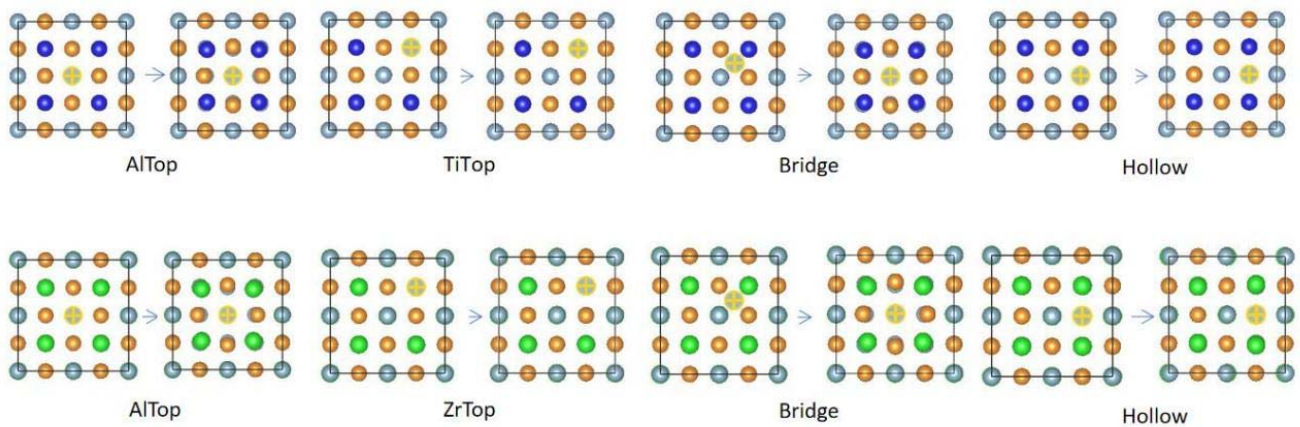

Figure 9. Initial and final sites of Al_3Ti (001) and Al_3Zr (001) for Al adsorption.

Table 8. Adsorption energies of Al on Al_3Ti (001) or Al on Al_3Zr (001) surfaces, initial and final site of adsorption, and distance between adsorption end and plane top layer.

Surfaces	Initial Site	D_{Al}-sur(Å)	E_{asd}(eV)	Final Site
Al_3Ti(001)	AlTop	1.67	−4.653	AlTop
	TiTop	2.34	−4.258	TiTop
	Bridge	1.63	−4.650	AlTop
	Hollow	1.85	−4.664	Hollow
Al_3Zr(001)	AlTop	1.96	−3.848	AlTop
	ZrTop	2.96	−2.303	ZrTop
	Bridge	1.96	−3.845	AlTop
	Hollow	2.37	−3.069	Hollow

3.8. Adsorption Energy of Al on Al_3Ti (112) or Al on Al_3Zr (114)

The dual nucleation theory is the most acceptable for the refinement mechanism consisting of forming a thin layer of Al_3Ti (112) on TiB_2 (0001) surface. Previous calculations suggested greater adhesion work between Al_3Zr (114) and TiB_2 (0001) than that between Al_3Ti (112) and TiB_2 (0001). As shown in Figure 10, the adsorption energies of Al on Al_3Ti (112) or Al on Al_3Zr (114) surfaces were calculated by selecting seven points for adsorption based on the complexity of Al_3Ti (112) and Al_3Zr (114) surfaces.
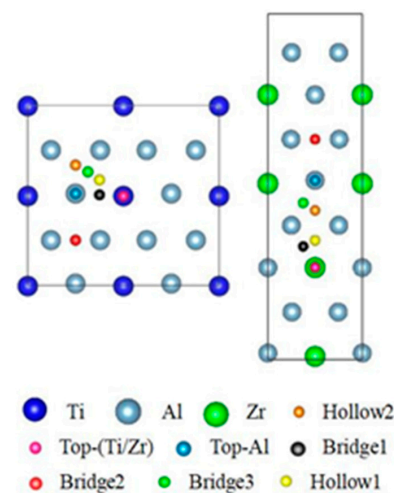

Figure 10. Surface structure and adsorption site of Al_3Ti (112) and Al_3Zr (114).

As shown in Figure 11, a total of seven adsorption points existed, with two sites at the top of Al atom and Ti atom. Three sites were selected at the bridge site: between Al-Ti atoms, between Al-Al atoms and away from Ti atoms, and between Al-Al atoms and close to Ti atoms. Hollow 1 was located at the center of Al-Al-Ti equilateral triangle, and hollow 2 was situated at the center of Al-Al-Al equilateral triangle. For adsorption of 7 sites, both the top and bridging sites crowded out the adjacent Al atoms to enter the hollow site after completion of the adsorption process.
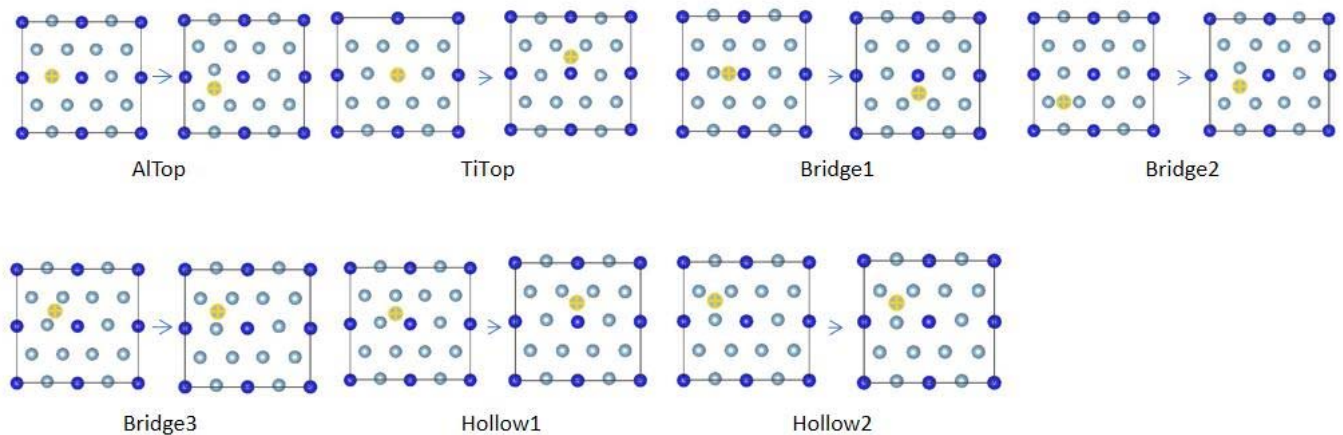

Figure 11. Initial and final site of Al on Al_3Ti (112) surface.

In Table 9, the highest adsorption energy was obtained at bridge site 2 with an energy of -23.204 eV. The secondary preferential adsorption was observed at the top of Al with energy of -23.202 eV. The energies of all sites were greater than 20 eV, and the adsorption energy of Al_3Ti (112) surface for Al atoms was about 4–5 times higher than that of Al_3Ti (001). Thus, Zr atoms existing in the melt led to significantly lower adsorption capacity for refining to Al. Similarly, the nucleation core with Al_3Zr (001)//Al_3Ti (001) mainly formed the crystal surface of Al (001) for growth and nucleation core with TiB_2 (0001)//Al_3Ti (112) as the base grown on Al (111) surface. Note that the surface energy of Al (001) was higher than that of Al (111). Al-related studies showed Al mainly nucleated with Al (111). As a result, Al (001) was more difficult to grow than Al (111).

Table 9. Adsorption energy of Al on Al_3Ti (112) surface, initial and final site of adsorption, and distance between adsorption end and plane top layer.

Surface	Initial Site	D_{Al}-sur(Å)	E_{asd}(eV)	Final Site
	AlTop	1.565	-23.202	Hollow2
	TiTop	2.007	-22.886	Hollow1
	Bridge1	1.984	-22.885	Hollow1
Al_3Ti(112)	Bridge2	1.528	-23.204	Hollow2
	Bridge3	2.185	-22.732	Hollow2
	Hollow1	1.940	-22.881	Hollow1
	Hollow2	2.177	-22.732	Hollow2

As shown in Figure 12, the initial and final site of the Al adsorption site of Al_3Zr (114) were the same as those of Al_3Ti (112), with the top site located above Al and Zr atoms. A total of three sites were selected for the bridge site, namely between Al-Zr atoms, between Al-Al atoms and away from Zr atoms, and between Al-Al atoms and close to Zr atoms. Hollow 1 was located at the center of Al-Al-Zr equilateral triangle, and hollow 2 was situated at the center of Al-Al-Al equilateral triangle. Except for bridge site 1 that remained at its location after completion of the adsorption, other adsorption ends moved toward the hollow site. The original hollow site may also crowd out nearby Al atoms to form a larger hollow.
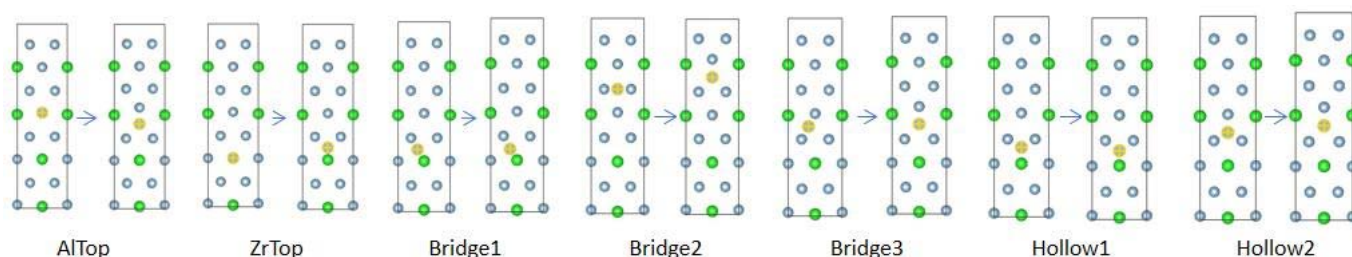
Figure 12. Initial and final site of Al on Al$_3$Zr (114) surface.

The adsorption energies of Al$_3$Zr (114) for Al are listed in Table 10. The most preferred adsorption point was based on hollow 2. The energy at the center of Al-Al-Al equilateral triangle was calculated to -23.695 eV, and the second was located at the top site directly above the Al atoms, thereby squeezing the Al atoms away to form a new hollow 2 with an energy of -23.058 eV. In general, hollow 2 can be considered as the optimal adsorption point. The highest adsorption energy of Al$_3$Zr (114) for Al was 0.491 eV superior, and the lowest adsorption energy was 0.579 eV inferior to that of Al$_3$Ti (112). However, the adsorption energy for Al atoms fluctuated between 22 and 23 eV when compared the whole, indicating both Al$_3$Ti (112) and Al$_3$Zr (114) surfaces with the same nucleation abilities in Al melt.

Table 10. Adsorption energy of Al on Al$_3$Zr (114) surface, initial and final site of adsorption, and distance between adsorption end and plane top layer.

Surface	Initial Site	D_{Al}-sur(Å)	E_{asd}(eV)	Final Site
	AlTop	1.391	-23.058	Hollow2
	ZrTop	2.169	-22.153	Hollow1
	Bridge1	2.188	-22.175	Bridge1
Al$_3$Zr(114)	Bridge2	1.364	-23.695	Hollow2
	Bridge3	1.418	-22.056	Hollow2
	Hollow1	2.219	-22.156	Hollow1
	Hollow2	1.427	-23.695	Hollow2

4. Conclusions

(1) For the first kind of Zr poisoning guess, the adhesion work relationship between ZrB$_2$ and Ti$_2$Zr with Al$_3$Ti (112) surface was calculated and the results showed lower values for ZrB$_2$ and Ti$_2$Zr than TiB$_2$ and Al$_3$Ti (112). The replacement of Ti by Zr revealed reduced binding of Al$_3$Ti (112), but the reduction was not significant.

(2) For the second kind of Zr poisoning guess, Al$_3$Zr in Zr containing melt showed a high melting point and was precipitated as Al$_3$Zr (001). The adhesion work between Al$_3$Zr (001) and Al$_3$Ti (001) was almost the same as that between TiB$_2$ (0001) and Al$_3$Ti (112), meaning that Al$_3$Ti (001) would accumulate on the Al3Zr (001) surface as precipitates. This agreed well with the experimental results reported by Xiao et al. [18]. The adsorption energy of Al on Al$_3$Ti (001) was only 1 / 5 ~ 1 / 4 of that of Al on Al$_3$Ti (112), and the energy required to form Al (001) surface was higher than that required to form Al (111). Hence, Al$_3$Zr (001) would compete with TiB$_2$ (0001) to seize Al$_3$Ti in the melt and then Al$_3$Ti (001) crystallized on Al$_3$Zr (001) surface. This seriously affected the condensation of Al, thereby reducing the probability of nucleation and producing Zr poisoning effect.

(3) For the third kind of Zr poisoning guess, Zr acted on Al$_3$Ti (112) of the TiB$_2$ surface. The calculations showed higher adhesion work of TiB$_2$//Al$_3$Zr (114) than that of TiB$_2$//Al$_3$Ti (112). Thus, Al$_3$Ti on the TiB$_2$ surface may be replaced by Zr, and TiB$_2$ could bind to Al$_3$Zr. However, the calculated adhesion work and adsorption energy of the Al$_3$Zr (114) surface to Al illustrated Al$_3$Zr (114) surface with almost the same effect as Al$_3$Ti (112). The adhesion work and adsorption energy were similar to those

of Al_3Ti (112). As a result, Zr may replace Ti, but its function remained the same as that of Ti without toxic effect.

References

1. Mi, L.; Wang, J.J.; Hu, Z.L. The Research Progress of TiB2 Impacts on the *Refin.* Effect of Al-Ti-B Master Alloy. *Appl. Mech. Mater.* **2014**, *3296*, 391–395. [CrossRef]
2. Wang, X.M.; Han, Q.Y. Grain Refinement Mechanism Of Aluminum by Al-Ti-B Master Alloys. In Proceedings of the Symposium on Light Metals Held during 145th The-Minerals-Metals-and-Materials-Society Annual Meeting and Exhibition, Nashville, TN, USA, 14–18 February 2016; pp. 189–193.
3. Cibula, A. The grain refinement of aluminum alloy castings by additions of titaniumand boron. *J. Inst. Met.* **1951**, *80*, 1.
4. Crossley, F.A.; Mondolfo, L.F. Mechanism of grain refinement in aluminum alloys. *JOM* **1951**, *3*, 1143–1148. [CrossRef]
5. Guzowski, M.M.; Sigworth, G.K.; Sentner, D.A. Role of boron in the grain refinement of aluminum with titanium. *Met. Trans. A (USA)* **1987**, *18a*, 603–619. [CrossRef]
6. Jones, G.P.; Pearson, J. Factors affecting the grain-refinement of aluminum using titanium and boron additives. *Metall. Trans. B* **1976**, *7*, 223–234. [CrossRef]
7. Qi, W.J.; Wang, S.C.; Chen, X.M.; Nong, D.; Zhou, Z. Effective nucleation phase and grain refinement mechanism of Al-5Ti-1B alloy. *China J. Rare Met.* **2013**, *37*, 179.
8. Fan, Z.; Wang, Y.; Zhang, Y.; Qin, T.; Zhou, X.R.; Thompson, G.E.; Pennycook, T.; Hashimoto, T. Grain refining mechanism in the Al/Al-Ti-B system. *Acta Mater.* **2015**, *84*, 292–304. [CrossRef]
9. Schumacher, P.; Greer, A.L.; Worth, J.; Evans, P.V.; Kearns, M.A.; Fisher, P.; Green, A.H. New studies of nucleation mechanisms in aluminium alloys: Implications for grain refinement practice. *Mater. Sci.Technol.* **1998**, *14*, 394–404. [CrossRef]
10. Mao, G.L.; Tong, G.Z.; Gao, W.L.; Liu, S.G.; Zhong, L.W. The poisoning effect of Sc or Zr in grain refinement of Al-Si-Mg alloy with Al-Ti-B. *Mater. Lett.* **2021**, *302*, 130428. [CrossRef]
11. Johnsson, M. Influence of Zr on the grain refinement of aluminium. *Metallkd* **1994**, *85*, 786–789. [CrossRef]
12. Zdziennicka, A.; Krawczyk, J.; Janczuk, B. Wettability and Adhesion Work Prediction in the Polymer-Aqueous Solution of Surface Active Agent Systems. *Colloids Interfaces* **2018**, *2*, 21. [CrossRef]
13. Wang, K.L.; Zhou, H.; Zhang, K.F.; Zhang, Y.S.; Feng, X.G.; Gui, B.H. A First-principles Study of Adhesion and Electronic Structure at TiN(111)/DLC Interface. *Rare Met. Mater. Eng.* **2021**, *50*, 2017–2024.
14. Liu, Y.; Huang, Y.C.; Xiao, Z.B.; Reng, X.W. Study of Adsorption of Hydrogen on Al, Cu, Mg, Ti Surfaces in Al Alloy Melt via First Principles Calculation. *Metals* **2017**, *7*, 21. [CrossRef]
15. Smith, A.E. Surface interface and stacking fault energies of magnesium from first principles calculations. *Surf. Sci.* **2007**, *601*, 5762–5765. [CrossRef]
16. Zeng, Q.Q.; Liu, Z.X.; Liang, W.F.; Ma, M.Y.; Deng, H.Q. A First-Principles Study on Na and O Adsorption Behaviors on Mo (110) Surface. *Metals* **2021**, *11*, 1322. [CrossRef]
17. Liu, S.Y.; Jiao, X.Q.; Zhang, G.Y. First principle study of the adsorption of formaldehyde molecule on intrinsic and doped BN sheet. *Chem. Phys. Lett.* **2019**, *726*, 77–82. [CrossRef]
18. Xiao, Z.B.; Deng, Y.L.; Tang, J.G.; Chen, Q.; Zhang, J.M. Poisoning mechanism of Zr on grain refiner of Al-Ti-C and Al-Ti-B. *Chin. J. Nonferrous Met.* **2012**, *22*, 371–379.

19. Liu, Q.B.; Fan, G.; Tan, Z.; Li, Z.; Zhang, D.; Wang, J.; Zhang, H. Precipitation of Al3Zr by two-step homogenization and its effect on the recrystallization and mechanical property in 2195 Al-Cu-Li alloys. *Mater. Sci. Eng. A Struct. Mater. Prop. Microstruct. Process.* **2021**, *821*, 141637. [CrossRef]

20. Wang, Y.; Fang, C.M.; Zhou, L.; Hashimoto, T.; Zhou, X.; Ramasse, Q.M.; Fan, Z. Mechanism for Zr poisoning of Al-Ti-B based grain refiners. *Acta Mater.* **2019**, *164*, 428–439. [CrossRef]